ЖУРНАЛ СТРУКТУРНОЙ ХИМИИ

2016. Том 57, № 4 *Май – июнь* *С. 822 – 830*

UDC 541.6:541.49:546.821

STRUCTURE AND PHOTOLUMINESCENCE PROPERTIES OF TiO_2 NANOPARTICLES SYNTHESIZED FROM A NOVEL LUMINESCENT NANO-TITANIUM COMPLEX

V. Jodaian[1], N.S. Langeroodi[2], E. Najafi[3]

[1]*Faculty of Science, Chemistry Department, Islamic Azad University, Islamshahr Branch, Iran*
E-mail: hvidajodaian@yahoo.co.nz.
[2]*Science Faculty, Chemistry Department, Golestan University, Gorgan, Iran*
[3]*Department of Chemistry, Payame Noor University (PNU), Tehran, Iran*

Received April, 6, 2015 *Revised — April, 29, 2015*

A new titanium complex $[Ti(Me—Q)_2(Cl)_2]$ (**1**) is prepared by reacting titanium tetrachloride with 2-methyl-8-hydroxyquinoline in a fast and facile process. The complex is fully characterized based on its ^1H and ^{13}C NMR, IR, and UV spectra and elemental analysis. The prepared nanostructured compound is synthesized by the sonochemical method. This new nanostructure is characterized by scanning electron microscopy (SEM), powder X-ray diffraction (XRD), IR spectroscopy, and elemental analysis. Thermal stability of single crystalline and nanosize samples of the prepared compound is studied by thermal gravimetric (TG) and differential thermal analysis (DTA). The prepared complexes both bulk and nanosized are utilized as a precursor for the preparation of TiO_2 nanoparticles by direct thermal decomposition at 600 °C in air. The morphology and size of TiO_2 nanoparticles are determined by SEM, powder XRD, and IR spectroscopy and the results show that the TiO_2 nanoparticle size depends on the initial particle size of **1**. Photoluminescence (PL) properties of the nanostructured and crystalline bulk prepared complex and their TiO_2 nanoparticle cores are investigated.

DOI: 10.15372/JSC20160423

K e y w o r d s: titanium complex, photoluminescence, size effect, TiO_2, Raman vibration.

INTRODUCTION

There continues to be great interest in combining proper ligands and metal ions to produce novel luminescent coordination compounds. This interest is not only due to their intrinsic architectural beauty or aesthetical structures but also the potential applications in the fields of organic light-emitting diodes (OLEDs), lasers, transistors, and fluorescent sensors for highly specific probes. Ligands and metal are a proper choice for attaining a good structural design and a strong application [1—5]. In recent years, many efforts have been devoted to understand the correlation between the electronic structure and the photonic properties of metal complexes of main and transition metal ions. In this context, the molecular structures and luminescent properties of large numbers of coordination compounds have been investigated [6—12]. On the other hand, the synthesis and design of novel luminescent nanostructured coordination compounds have been subject to rapid growth in recent years because of their unique electronic, magnetic, and optical properties [13—16]. It is well documented that the chemical and physical properties of materials with morphological features smaller than a micron in at least one dimension, i.e. nanomaterials, differ from the properties of their bulk morphologies due to their small size and large surface-to-volume ratios [17—19]. Therefore, nanosized coordination

supramolecular materials are interesting candidates for applications in many fields, including catalysis, molecular adsorption, magnetism, nonlinear optics, luminescence, and molecular sensing [20—24]. The properties of nanomaterials, especially the photoluminescent properties, have been a subject of extensive investigations. There are a range of methods to produce metallic nanosized materials, including radiation methods, thermal decomposition, chemical vapor deposition, reduction in microemulsions, and chemical reduction methods [25—30]. However, most of these techniques tend to be expensive and time-consuming. Therefore, the development of an alternative route for the preparation of high-quality metallic nanosized materials should be beneficial. In this work, a uniform nanotitanium complex was prepared by a simple and cost-effective method, the sonochemical method, for the first time. Ultrasound has been very useful in the synthesis of a wide range of nanostructured materials, including high-surface area transition metals, alloys, carbides, oxides, and colloids. The chemical effects of ultrasound do not come from a direct interaction with molecular species. Instead, sonochemistry arises from acoustic cavitation: the formation, growth, and implosive collapse of bubbles in a liquid. Cavitational collapse produces intense local heating (~5000 K), high pressures (~1000 atm), and enormous heating and cooling rates (>10^9 K/s).

To our knowledge, the relationship between the size of nanostructured coordination compounds and the emission wavelength has not been reported. In order to study the effect of the size of nanostructured coordination compounds on their optical properties, we report here the synthesis and characterization of a new titanium complex with an O- and N-donor ligand (2-methyl-8-hydroxyquinolate) as nanostructured and crystalline bulk. Also, the photoluminescent properties of the prepared compounds and the particle size effect on their photophysical properties have been investigated. The nanostructured and crystalline bulk of the prepared complex were utilized as a precursor for the preparation of TiO_2 nanoparticles by direct thermal decomposition at 600 °C in air.

EXPERIMENTAL

Materials and physical techniques. 2-Methyl-8-hydroxyquinoline was obtained from Merck and used without further purification. $TiCl_4$ (Merck) was freshly distilled prior to use. The melting point was determined with an Electrothermal 9200 melting point apparatus and was not corrected. All manipulations were performed under a dry nitrogen atmosphere using the standard Schlenk line technique. All solvents were dried and distilled under nitrogen prior to use, according to the standard procedure [31]. Infrared spectra were measured in the range 4000—250 cm^{-1} on a Bomem MB-series FT-IR instrument, using KBr pellets. NMR spectra were recorded at room temperature in DMSO on Bruker AVANCE 300 MHz operating at 300.3 MHz. Elemental analysis was performed with a Thermo vario El microanalyzer. The photoluminescence spectra were obtained on a USB2000 spectrometer. UV-Vis spectra were recorded on a Shimadzu 2100 spectrometer. The solid state fluorescence quantum yields of the titanium complexes were calculated using an optical power meter. The thermal analysis (TG-DTA) was carried out on a Bahr STA-503 instrument in the air atmosphere. The XRD pattern was obtained on a STOE diffractometer with CuK_α radiation. The morphology and structure investigations were performed by SEM on KYKY-EM3200 with 25 kV accelerating voltage.

Preparation of complexes. Preparation of [Ti(Me-Q)$_2$(Cl)$_2$]. For the preparation of the title compound, to a solution of 2-methyl-8-hydroxyquinolin (0.32 g, 2 mmol) in 15 ml of methanol, $TiCl_4$ (0.11 ml, 1 mmol) was added at room temperature. The above solution under stirring gave a yellow-orange solid. The solid was filtered off, washed with methanol, and dried (yield 78 %, m.p. > 270 °C). Anal. Calc. for $C_{21}H_{20}Cl_2N_2O_3Ti$ (%): C 53.99, H 4.32, N 6.00. Found (%): C 54.22, H 4.45, N 6.09. IR (KBr, cm^{-1}): 3030 (w), 2994 (w), 1458 (m), 452 (m), 528 (m). ^{1}H NMR (DMSO): δ 2.85 (6H, CH_3—HQ), 3.21 (3H, CH_3OH), 7.13, 7.18, 7.72, 7.93, 8.51 (10H, HQ—H). ^{13}C NMR (DMSO): δ 25.4 (CH_3—HQ), 44.2 (CH_3OH), 113.2, 116.3, 123.7, 127.4, 129.7, 134.8, 137.2, 151.4, 154.8 (Ar—C). Finally, TiO_2 nanostructures were prepared by calcination of compound **1** at 600 °C in a furnace and a static air atmosphere for 4 h.

Preparation of nanosized 1 by the sonochemical method. For the preparation of nanosized **1**, a solution of 2-methyl-8-hydroxyquinolin (0.32 g, 2 mmol) in methanol was transferred in a high-

density ultrasonic probe. To this solution a $TiCl_4$ solution (0.11 ml, 1 mmol) in methanol was added dropwise. The obtained precipitates were filtered, subsequently washed with methanol and then dried in air (yield 85 %, m.p. > 270 °C). Anal. Calc. for $C_{21}H_{20}Cl_2N_2O_3Ti$ (%): C 53.99, H 4.32, N 6.00. Found (%): C 54.24, H 4.38, N 6.07. IR (KBr, cm^{-1}): 3030 (w), 2998 (w), 1464 (m), 452 (m), 528 (m). Finally, in order to obtain TiO_2 nanostructures, fine powder of nanostructured compound **1** was calcined at 600 °C in a furnace and a static air atmosphere for 4 h.

RESULTS AND DISCUSSION

Scheme 1 gives an overview of the methods used for the synthesis of the nanostructured and crystalline bulk of the prepared complex and their conversion to TiO_2 by calcination.

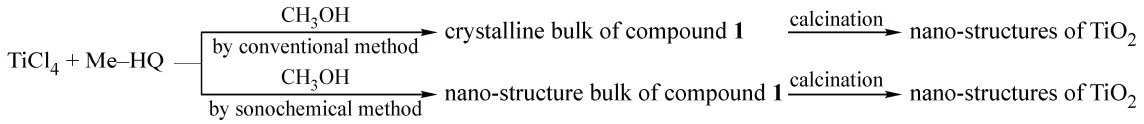

Scheme 1. Materials produced from the reaction of the 2-methyl-8-hydroxyquinoline ligand with titanium tetrachloride by two different methods and the fabrication of TiO_2

It was found that the reaction of 2-methyl-8-hydroxyquinoline and titanium tetrachloride in dry methanol led to the formation of single crystals of the synthesized complex. In the present study, a simple and cost-effective methodology (the sonochemical method) was used to synthesize a nanotitanium complex of 2-methyl-8-hydroxyquinoline. In this method, molecules are promoted to form nanosized particles by the application of powerful ultrasound radiation (e.g., 20 kHz—10 MHz), which results in a practically instantaneous formation of a plethora of crystallization nuclei [32]. The new method is straightforward and cheap and provides a clean reaction for the preparation of nanocoordinated polymers without any side product.

These reactions are fast, facile and their progress was monitored by the appearance of fluorescent colors. The elemental analyses and IR data for both compounds are in accordance with the formula $[Ti(Me—Q)_2(Cl)_2]$. Spectroscopic data for both complexes are similar, which indicates that they have similar structures. Notably, both complexes are stable at room temperature and can be stored at room temperature for an indefinite period of time. The good stability of the complexes is probably associated with the overall molecule linked together by covalent Ti—O bonds, thus providing the adequate thermodynamic stability for the existence in the solid state.

General characterization. In general, FT-IR spectroscopy has been shown to be a powerful tool for extracting structural information on the molecules. The IR spectra of both complexes are similar, which indicates that they have similar structures. The IR spectra of the prepared compounds have a medium broad peak in the highest frequency range, which was assigned to an aromatic C—H bond appearing in the range 2930—3000 cm^{-1}, and the bands observed in the range 3000—3050 cm^{-1} are related to methyl C—H groups. The broad band centered at ca. 3550—3600 cm^{-1} indicates the O—H stretching of the lattice methanol molecules. The bands observed in the range 1600—1380 cm^{-1} are assigned to C=N and C=C stretching vibrations. In comparison with the free ligand, the new bands at about 528 and 452 cm^{-1} were assigned to Ti—N and Ti—O vibrations, respectively, which proves the coordination of nitrogen and oxygen to titanium. The Ti—N and Ti—O stretching vibrations appear at frequencies similar to those observed in other titanium complexes [33]. The IR spectrum of the nanostructured prepared complex is identical with the spectrum of the single crystalline material, which indicates that they have similar structures.

For the determination of the structural features of the prepared compounds in solution, attempts were made to record the ^1H and ^{13}C NMR spectra of the prepared complexes. The ^1H NMR spectrum of the prepared complex (Scheme 2) shows the expected aromatic peaks with the correct integration.

In the ^1H NMR spectra of the prepared complex, the ligand signals are generally displaced to lower fields. This is likely to be due to the coordination of the 2-methyl-8-hydroxyquinolate ligand to

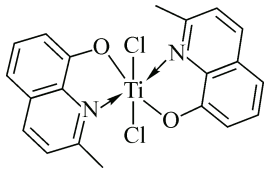

Scheme 2. Line drawing structure of the complex

Ti(IV) and the formation of Ti—N and Ti—O bonds. The shift is a consequence of an electron density transfer from the ligand to the acceptor. The observed signals in the range 7.13—8.51 ppm are related to aromatic protons of the 2-methyl-8-hydroxyquinolate ligand. The signal observed around 2.85 ppm is related to methyl group protons of the 2-methyl-8-hydroxyquinolate ligand.

In the ^{13}C NMR spectrum of the prepared complex, which is generally consistent with the conclusions drawn from the ^{1}H NMR results, the ligand signals are only slightly shifted from their positions in the spectrum of the free donor ligand, which could be attributed to the coordination of the 2-methyl-8-hydroxyquinolate ligand to Ti(IV).

In order to evaluate the role of the sonochemical method in the synthesis of nanostructured complex **1**, a Tecna ultrasonic bath was used to prepare nanosized **1**. Fig. S1, *a* shows the XRD pattern of the crystalline bulk of the prepared complex, and Fig. S1, *b* shows the XRD pattern of a typical sample of $[Ti(Me—Q)_2(Cl)_2]$ (**1**) prepared in the ultrasonic bath. Acceptable matches, with slight differences in 2θ, were observed between the XRD patterns of the nanostructured and crystalline bulk of the prepared complex. These data confirm that the obtained compound is one crystalline phase. Estimated from the Scherrer formula for the calculation of particle sizes from the broadening of the XRD peaks ($D = 0.891\ k/b\ \cos\theta$, where D is the average grain size, k is the X-ray wavelength (0.15406 nm), and θ and b are the diffraction angle and full-width at half maximum (FWHM) of an observed peak, respectively), the average size of the particles was found to be around 56 and 335 nm for the nanostructured and crystalline bulk of the prepared complex.

The size and morphology of the nanostructured and crystalline bulk of the prepared complex were examined by SEM. The SEM images, as shown in Fig. S2, reveal that the prepared compounds both single crystals and nanoparticles, have sphere-like morphology with an average diameter of about 320 and 47 nm, respectively.

TGA and DTA were carried out between 0 and 850 °C in the static air atmosphere to study the behavior of the nanostructured and crystalline bulk of the prepared complex during heat treatment (Figs. S3 and S4). Single crystals of the synthesized complex are stable to ca. 95 °C. The first mass loss between 85 and 105 °C in TGA, which is accompanied by an endothermic peak in the DTA curve, is due to the loss of lattice methanol molecules. The distinct mass loss from 430 to 650 °C in TGA is attributed to the elimination of Me—HQ ligands. The solid precipitate formed around 700 °C is probably TiO_2. Nanoparticles of the prepared complex are less stable and start to decompose at 405 °C. The decomposition of the prepared nanosized complex starts at about 25 deg. earlier (Fig. S3, *b*) than that of its single crystals, probably due to the reduction of the particle size of the complexes to a few dozen nanometers, which results in lower thermal stability as compared to the single crystal samples. For single crystals of the synthesized compound the DTA curve displays a broad exothermic peak at 515 °C (Fig. S4). The DTA curve of the nanostructured material has the same general appearance as those of their single crystal counterpart and the exo- and endothermic peaks are retained for the nanostructured complex (Fig. S4, *a*, *b*). In agreement with TGA results, some differences between the maximum intensities confirm the lower thermal stability of the nanostructures in comparison with single crystals of the prepared complex.

Optical properties of the prepared complex. The exploration of novel properties of nanocrystalline materials, especially the photoluminescent properties, has been the subject of extensive investigations for some time. For nanocrystalline materials the quantum confinement effect is expected. Nanocrystalline materials with dimensions less than 100 nm exhibit the new and interesting size-

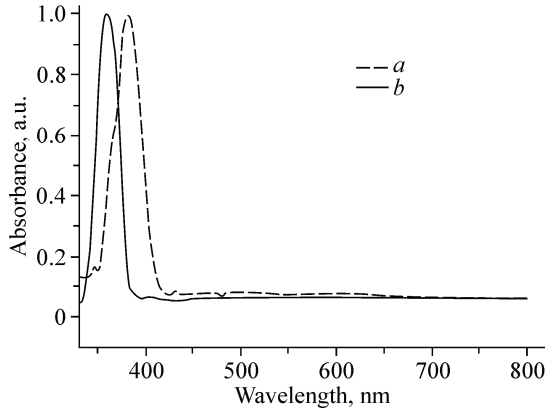

Fig. 1. Absorption spectra of the complex: single crystals (*a*) and nanostructures (*b*)

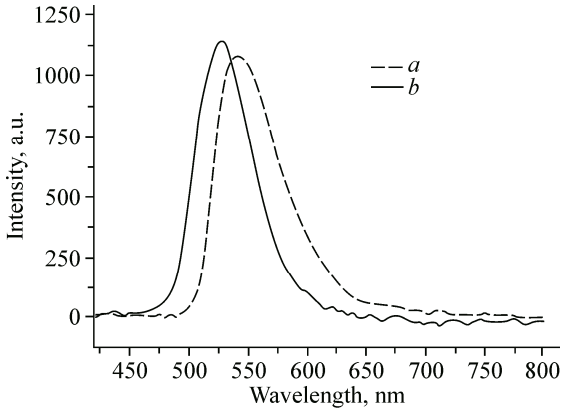

Fig. 2. Fluorescence spectra of the complex: single crystals (*a*) and nanostructures (*b*)

dependent physical and chemical properties that cannot be observed in bulk analogues. In nanocrystalline materials, band gaps have been found to be particle size dependent [34]. In order to confirm this, the solid state absorption spectra of the nanostructured and crystalline bulk of the prepared complex and the particle size effect on its photophysical properties have been investigated and the results are depicted in Fig. 1.

The crystalline bulk of the prepared complex demonstrates an absorption peak centered at 382 nm as compared to that at 356 nm in the prepared nanostructured complex. There is a 26 nm blue-shift for the absorption spectrum of the prepared nanostructured complex relative to the crystalline bulk of the prepared complex due to the quantum confinement effect. The maxima of the absorption peaks show that there is good correlation between the particle size and their absorption wavelengths. As can be seen, the emission wavelengths of the titanium complexes are dependent on their size. When the particle size decreases, the effective band gap increases, therefore, the emitted photon has a comparatively higher energy giving a photoluminescence peak at a shorter wavelength [35]. Notably, the absorption spectra of the nanostructured and crystalline bulk of the prepared complex have similar shapes. Therefore, one can conclude that the absorption peak of both compounds originates from $\pi \rightarrow \pi^*$ transitions of the aromatic rings [36]. The energy gap of the nanostructured and crystalline bulk of the prepared complex has been determined by the absorption edge of the UV-absorption spectra [37]. The absorption onset of compounds as single crystals (*a*) and as nanostructures (*b*) is 408 and 386 nm, respectively. The absorption onset is red shifted upon particle growth, indicating that the particles are really in the quantum regime. In this work, the band gap value found for the prepared nanostructured complex (3.21 eV) is larger than that of the crystalline bulk of the prepared complex (3.03 eV).

The solid state emission spectra of the compounds are collected from 440 to 800 nm. The photoluminescence spectra of the prepared compounds are shown in Fig. 2.

The prepared compound as nanoparticles (*b*) shows a blue shift in comparison with that of the single crystal (*a*). As shown in Fig. 2, the compound (*a*) demonstrates broad photoluminescence emission centered at 537 nm as compared to the compound (*b*) at 525 nm. Thus, there is a 12 nm blue-shift for the emission spectrum of the compound (*b*) relative to the compound (*a*).

The solid-state fluorescence absolute quantum yields for the single crystal and nanoparticles are obtained as 0.68 and 0.77, respectively, as described by Moreno [38]. According to the quantum yields and fluorescence spectra of the prepared complexes, all complexes have relatively good fluorescent properties. As can be seen, a definite particle size effect is observed. Importantly, the maximum quantum yield of the nanostructured and crystalline bulk of the prepared complex shows a similar size effect to the photoluminescence of these compounds: a higher quantum yield for the prepared nanostructured complex and a lower quantum yield for the crystalline bulk of the prepared complex. Considering the above mentioned points together with the relevant results of solid UV-Vis and PL measurements, we believe that the prepared complex can be used as a potential material for light emitting diode devices and be a candidate for thermally stable and solvent-resistant fluorescent material.

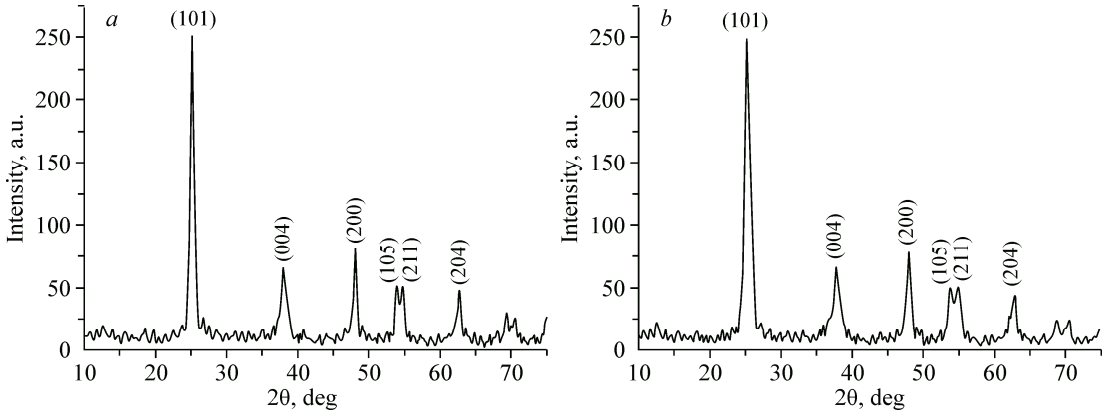

Fig. 3. XRD patterns; TiO_2 prepared by calcination of the crystalline bulk of the prepared complex at 600 °C(*a*) and TiO_2 prepared by calcination of the nanostructured complex at 600 °C (*b*)

Preparation of titanium dioxide from the nanostructured and crystalline bulk of the prepared complex. Semiconductor nanoparticles have a wide range of applications in various fields, such as microelectronics, photocatalysis, nonlinear optics, photoelectrochemistry, imaging science, and electro-optics [39, 40]. Among various semiconductor materials, TiO_2 possesses interesting optical, dielectric, and catalytic properties. Titanium dioxide (TiO_2) has been widely used in many applications such as pigments, adsorbents, and catalytic supports. This material also possesses many advantages such as (i) high photochemical stability in air (ii) low cost, and (iii) possibility of the introduction of dopants to enhance the sensitivity or selectivity [41—43]. Until now, considerable effort has been dedicated to the controlled synthesis of nanoscale TiO_2 particles with different morphological configurations and size distributions [44—46]. However, the use of metal organic compounds as precursors for the preparation of nanomaterials such as TiO_2 has not yet been thoroughly investigated. The preparation of TiO_2 by wet chemical methods, such as sol-gel, precipitation, and the hydrothermal method, usually results in the formation of agglomerated TiO_2 powder with a wide-diameter distribution. Therefore, the development of a fast and efficient method to produce high-quality TiO_2 nanoparticles and control the crystal size is a new challenge for synthetic chemists and materials scientists. In this paper, we have developed a simple calcination method for the preparation of TiO_2 nanoparticles. In this study it has been demonstrated that supramolecular compounds can be suitable precursors for the preparation of nanoscale materials.

The structure of TiO_2 nanoparticles prepared by direct calcination of the crystalline bulk of the prepared complex at 600 °C is shown in Fig. 3, *a*. A comparison of this data with the JCPDS files (No. 21-1272) indicates that the diffraction peaks are consistent with a tetragonal crystal system having an $I41/amd$ space group and lattice parameters $a = 3.7852$ Å and $c = 9.5139$ Å and $Z = 4$. There is no unknown peaks in the XRD pattern. The morphology and size of the titanium dioxide nanoparticles produced by direct calcination of the crystalline bulk of the prepared complex was studied by SEM. A SEM image (Fig. 4, *a*) of the precipitate shows that the particles have a good size distribution and

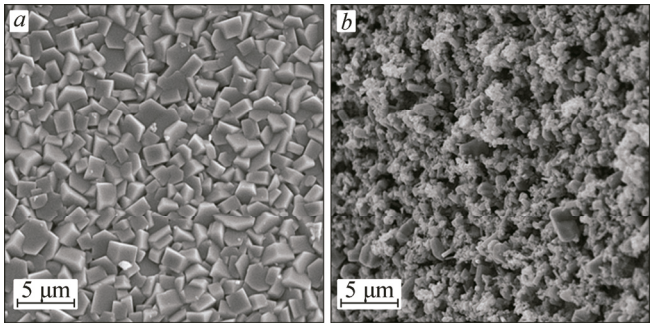

Fig. 4. SEM images of TiO_2 prepared by calcination of the crystalline bulk of the prepared complex at 600 °C (*a*) and TiO_2 prepared by calcination of the nanostructured complex at 600 °C (*b*)

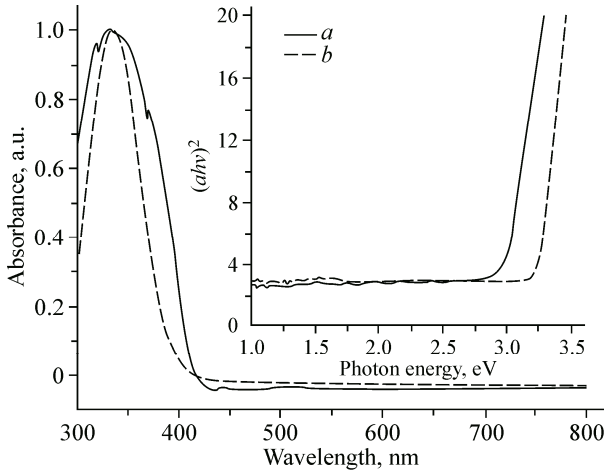

Fig. 5. UV-Vis absorption spectra; TiO_2 prepared by calcination of the crystalline bulk of the prepared complex at 600 °C (*a*) and TiO_2 prepared by calcination of the nanostructured complex at 600 °C (*b*) (The inset shows the $(\alpha(h\nu))^2$ *versus* the photon energy curve)

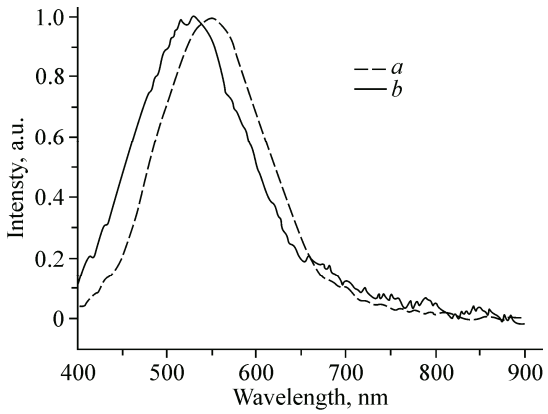

Fig. 6. Photoluminescence spectra; TiO_2 prepared by calcination of the crystalline bulk of the prepared complex at 600 °C (*a*) and TiO_2 prepared by calcination of the nanostructured complex at 600 °C (*b*)

good particle separation with an average diameter of about 70 nm. Since the calcination process was successful for the preparation of TiO_2 nanoparticles, the nanostructured complex was prepared by the sonochemical process to obtain TiO_2 nanoparticles. The XRD pattern (Fig. 3, *b*) of the TiO_2 nanoparticles prepared by direct calcination of the nanostructured complex shows that the resulting precipitate possesses the same structure as the TiO_2 nanoparticle obtained from the crystalline bulk of the prepared complex with the same lattice parameters as mentioned above. The SEM image of the resulting precipitate shows that the TiO_2 nanoparticles have a good size distribution with an average diameter of 43 nm (Fig. 4, *b*). These results indicate that good correlation exists between the size of the coordination compound precursor and the size of the nanoparticles formed and that the nano-sized precursor produces smaller TiO_2 particles.

Optical properties of TiO_2 nanoparticles. It has been reported that the band gap of a crystalline semiconductor is a function of the particle size [47—49]. In order to confirm this, the absorption spectrum was measured from the TiO_2 nanoparticles prepared by direct calcination of the nanostructured and crystalline bulk of the prepared complex at 600 °C, and the results are depicted in Fig. 5. The absorption onset of TiO_2 prepared by calcination of the nanostructured and crystalline bulk of the prepared complex at 600 °C is 379 and 413 nm, respectively. The absorption onset appears to be red shifted upon particle growth, indicating that the particles are indeed in the quantum regime. The optical absorbance coefficient α of a semiconductor close to the band edge can be expressed as $\alpha(h\nu) \propto \propto (h\nu - Eg)^{1/2}/h\nu$ [50], where α is the absorption coefficient, *Eg* is the absorption band gap, $h\nu$ is the photon energy, *n* depends on the nature of transitions, $n = 1/2$ for the direct band gap transitions, $n = 2$ for the indirect band gap transitions. In this case, $n = 1/2$ for direct transitions. Plots of $(\alpha(h\nu))^2$ *versus* $h\nu$ can be derived from the absorption data in Fig. 5. The intercept of the tangent to the plot gives a good approximation of the band gap energy of the direct band gap materials (shown in the inset in Fig. 5 for TiO_2 from the nanostructured and crystalline bulk of the prepared complex). The band gap of TiO_2 prepared by calcination of compounds as single crystals (*a*) and as nanoparticles (*b*) is 3 and 3.25 nm, respectively. The band gap of TiO_2 nanoparticles prepared by calcination of the nanostructured complex is larger than that of TiO_2 nanoparticles prepared by calcination of the crystalline bulk of the prepared complex due to the quantum size effect.

The PL spectrum of the TiO_2 nanoparticles measured at room temperature is given in Fig. 6. The PL spectra of TiO_2 nanoparticles prepared by calcination of the nanostructured and crystalline bulk of the prepared complex exhibit bands at 534 and 548 nm, respectively, which can be attributed to the

direct recombination between electrons in the conduction band and holes in the valence band. As can be seen, similarly to the PL properties of the nanostructured and crystalline bulk of the prepared complex, the emission wavelengths of titanium dioxide nanoparticles are dependent on their size.

Raman vibrational properties of TiO_2 nanoparticles. For semiconductor nanoparticles, the quantum confinement effect is expected. Semiconductor nanoparticles with dimensions of the order of the bulk exciton will show unique properties which strongly depend on the size. As the particle size decreases, The Raman peaks show an increased broadening and systematic frequency shifts. The vibrational spectrum of TiO_2 nanoparticles exhibit six Raman-active fundamentals (Fig. S5): three *Eg* modes centered around 146, 194, and 645 cm^{-1}, two *B*1*g* modes at 399 and 519 cm^{-1}, and an *A*1*g* mode at 513 cm^{-1}. The most intense *Eg*(1) mode shows a significant broadening with decreasing crystallite size. The *B*1*g*(1) mode and the *B*1*g*(2)+*A*1*g* modes show very small blue and red shifts, respectively, while a small blue shift is seen for the *Eg*(2) mode. The *Eg*(3) mode shows a significant broadening and a red shift with decreasing crystallite size.

CONCLUSIONS

In summary, a new Ti(IV) complex $[Ti(Me—Q)_2(Cl)_2]$ (**1**) was synthesized and characterized by spectroscopic methods. The nanostructured complex was obtained by the sonochemical process. This study shows that the emission wavelength of the Ti(IV) complexes can be tuned in the solid state over a wide wavelength range by changing the size of the complex particles. Interestingly, the absorption and emission peaks of the crystalline bulk of the prepared complex were found to be significantly red shifted in comparison with those of the prepared nanostructured complex. TiO_2 nanoparticles were synthesized in a simple one-pot calcination of the nanostructured and crystalline bulk of the prepared complex. The morphology and size of the TiO_2 nanoparticles were determined, and the results showed that particle size and morphology of the TiO_2 nanoparticle depend on the initial particle size of **1**. The photoluminescence (PL) properties of the nanostructured and crystalline bulk of the prepared complex and their TiO_2 nanoparticle core in the solid state were investigated in detail at room temperature. The results indicate that the particle size has an important effect on their optical properties. It is also interesting to note that the prepared nanostructured complex is the first sample prepared by the sonochemical method as an alternative to the synthetic procedure to obtain nanosized particles of a coordination polymer. This preparation method can have advantages such as short reaction times, higher yields and can also produce nanosized particles of the coordination polymer. In our laboratory, we have focused our efforts on the preparation of other coordination compound with different metal ions by the sonochemical method. We anticipate that this method would provide new insights into metal-organic supramolecular assembly and nanochemistry.

The authors thank the Vice-President′s Office for Research Affairs of Islamic Azad University, Islamshahr Branch for supporting this work.

REFERENCES

1. *Shinar J*. Organic light-emitting devices. – New York: Springer, 2003.
2. *Miller R.D., Chandross E.A*. // Chem. Rev. – 2010. – **110**. – P. 1 – 2.
3. *Koch N*. // Chem. Phys. Chem. – 2007. – **8**. – P. 1438 – 1455.
4. *Holm R.H., O'Connor M.J*. // Prog. Inorg. Chem. – 1971. – **14**. – P. 241 – 401.
5. *Garnovskii A.D., Nivorozhkin A.L., Minkin V.I*. // Coord. Chem. Rev. – 1993. – **126**. – P. 1 – 69.
6. *Qin Y., Pagba C., Piotrowiak P., Jakle F*. // J. Am. Chem. Soc. – 2004. – **126**. – P. 7015 – 7018.
7. *Brinkmann M., Fite B., Pratontep S., Chaumont C*. // Chem. Mater. – 2004. – **16**. – P. 4627 – 4633.
8. *Shavaleev N.M., Adams H., Best J., Edge R., Navaratnam S., Weinstein J.A*. // Inorg. Chem. – 2006. – **45**. – P. 9410 – 9415.
9. *Hamada Y., Sano T., Fujita M., Fujii T., Nishio Y., Shibata K*. // Jpn. J. Appl. Phys. – 1993. – **32**. – P. L511 – L513.
10. *Kim S.M., Kim J.S., Shin D.M., Kim Y.K., Ha Y*. // Bull. Korean. Chem. Soc. – 2001. – **22**. – P. 743 – 747.
11. *Wang P.F., Hong Z.R., Xie Z.Y., Tong S.W., Wong O., Lee C.S., Wong N.B., Hung L.S., Lee S.T*. // Chem. Commun. – 2003. – **14**. – P. 1664 – 1665.

12. *Yu T., Su W., Li W., Hong Z., Hua R., Li M., Chu B., Li B., Zhang Z., Hu Z.Z.* // Inorg. Chim. Acta. – 2006. – **359**. – P. 2246 – 2251.
13. *Shi H.T., Qi L.M., Ma J.M., Cheng H.M.* // J. Am. Chem. Soc. – 2003. – **125**. – P. 3450 – 3451.
14. *Zhang H., Yang D.R., Li D.S., Ma X.Y., Li S.Z., Que D.L.* // Cryst. Growth Des. – 2005. – **5**. – P. 547 – 550.
15. *Kuang D.B., Xu A.W., Fang Y.P., Liu H.Q., Frommen C., Fenske D.* // Adv. Mater. – 2003. – **15**. – P. 1747 – 1750.
16. *Kim F., Connor S., Song H., Kuykendall T., Yang P.D.* // Angew. Chem., Int. Ed. – 2004. – **43**. – P. 3673 – 3677.
17. *Chen J., Herricks T., Xia Y.* // Angew. Chem., Int. Ed. – 2005. – **44**. – P. 2589 – 2592.
18. *Horn D., Rieger J.* // Angew. Chem., Int. Ed. –2001. – **40**. – P. 4330 – 4361.
19. *Shen X.F., Yan X.P.* // Angew. Chem., Int. Ed. – 2007. – **46**. – P. 7659 – 7663.
20. *Zhang D.E., Zhang X.J., Ni X.M., Zheng H.G., Yang D.D.* // J. Magn. Magn. Mater. – 2005. – **292**. – P. 79 – 82.
21. *Wang J., Gudiksen M.S., Duan X., Cui Y., Lieber C.M.* // Science. – 2001. – **293**. – P. 1455 – 1457.
22. *Lu W., Qin X., Luo Y., Chang G., Sun X.* // Microchim. Acta. – 2011. – **175**. – P. 355 – 359.
23. *Bruchez M., Moronne M., Gin P., Weiss S., Alivisatos A.P.* // Science. – 1998. – **281**. – P. 2013 – 2016.
24. *Mirkin C.A., Letsinger R.L., Mucic R.C., Storhoff J.J.* // Nature. – 1996. – **382**. – P. 607 – 609.
25. *Yeh M.S., Yang Y.S., Lee Y.P., Lee H.F., Yeh Y.H., Yeh C.S.* // J. Phys. Chem. B. – 1999. – **103**. – P. 6851 – 6857.
26. *Shahriari E., Yunus W.M.M., Saion E.* // Braz. J. Phys. – 2010. – **40**. – P. 256 – 260.
27. *Ponce A.A., Klabunde K.J.* // J. Mol. Catal. A.: Chem. – 2005. – **225**. – P. 1 – 6.
28. *Iranpoor N., Firouzabadi H., Safavi A., Motevalli S., Doroodmand M.M.* // Appl. Organomet. Chem. – 2012. – **26**. – P. 417 – 424.
29. *Kowlgi K., Lafont U., Rappolt M., Koper G.* // J. Colloid Interface Sci. – 2012. – **372**. – P. 16 – 23.
30. *Khan Z., Al-Thabaiti S.A., Obaid A.Y., Al-Youbi A.O.* // Colloids Surf. B. – 2011. – **82**. – P. 513 – 517.
31. *Perrin D.D., Armarego W.L.F., Perrin D.R.* Purification of Laboratory Chemicals. – 2nd ed. – New York: Springer, 1980.
32. *Suslick K.S., Choe S.B., Cichowlas A.A., Grinstaff M.W.* // Nature. – 1991. – **353**. – P. 414 – 416.
33. *Zeng W.F., Chen Y.S., Chiang M.Y., Chern S.S., Cheng C.P.* // Polyhedron. – 2002. – **21**. – P. 1081 – 1087.
34. *He J.H., Wu T.H., Hsin C.L., Li K.M., Chen L.J., Chueh Y.L., Chou L.J., Wang Z.L.* // Small. – 2006. – **2**. – P. 116 – 120.
35. *Gupta P., Ramrakhiani M.* // Open Nanosci. J. – 2009. – **3**. – P. 15 – 19.
36. *Huang J., Wang X., Jacobson A.J.* // J. Mater. Chem. – 2003. – **13**. – P. 191 – 196.
37. *Jiang P., Zhu W., Gan Z., Huang W., Li J., Zeng H., Shi J.* // J. Mater. Chem. – 2009. – **19**. – P. 4551 – 4556.
38. *Moreno L.A.* // J. Visualized Exp. – 2012. – **63**. – P. e3066. – doi: 10.3791/3066.
39. *Juarez A.S., Ortiz A.* // J. Electrochem. Soc. – 2000. – **147**. – P. 3708 – 3717.
40. *Nehru L.C., Swaminathan V., Sanjeeviraja C.* // Am. J. Mater. Sci. – 2012. – **2**. – P. 6 – 10.
41. *Ramakrishna G., Ghosh H.N.* // Langmuir. – 2003. – **19**. – P. 505 – 508.
42. *Rahman M.M., Krishna K.M., Soga T., Jimbo T., Umeno M.* // J. Phys. Chem. Solids. – 1999. – **60**. – P. 201 – 210.
43. *Pelizzetti E., Minero C.* // Elecrochim. Acta. – 1993. – **38**. – P. 47 – 55.
44. *Li B., Wang X., Yan M., Li L.* // Mater. Chem. Phys. – 2002. – **78**. – P. 184 – 188.
45. *Kolenko Y., Churagulov B.R., Kunst M., Mazerolles L., Colbeau-Justin C.* // Appl. Catal. B. – 2004. – **54**. – P. 51 – 58.
46. *Zhou W., Cao Q., Tang S.* // Powder Technol. – 2006. – **168**. – P. 32 – 36.
47. *Kowshik M., Vogel W., Urban J., Kulkarni S.K., Paknikar K.M.* // Adv. Mater. – 2002. – **14**. – P. 815 – 818.
48. *Xiong S.L., Xi B.J., Xu D.C., Wang C.M., Feng X.M., Zhou H.Y., Qian Y.T.* // J. Phys. Chem. C. – 2007. – **111**. – P. 16761 – 16767.
49. *Liu X., Wu X., Cao H., Chang R.P.H.* // J. Appl. Phys. – 2004. – **95**. – P. 3141 – 3147.
50. *Mills G., Li Z.G., Meisel D.* // J. Phys. Chem. – 1988. – **92**. – P. 822 – 828.